COBEM 2023 27TH INTERNATIONAL CONGRESS OF MECHANICAL ENGENEERING

ABCM Brazilian Society of Mechanical Sciences and Engineering
27th ABCM International Congress of Mechanical Engineering
December 04-08, 2023, Florianópolis-SC, Brazil

COB-2023-1516
THE APPLICATION OF MAGNETO-RHEOLOGICAL ELASTOMER IN A BASE INSOLATION SYSTEM FOR SEISMIC MITIGATION OF HIGHWAY BRIDGES

Fernanda Carolina de Almeida
Matheus Silva Proença
Henrique Edno Leoncini de Carvalho
Daniel Henrique de Sousa Obata
Jeferson Camargo Fukushima
Amarildo Tabone Paschoalini
Sao Paulo State-University (Unesp) – School of Engineering, Ilha Solteira-SP, Brazil.
f.almeida@unesp.br, matheus.proenca@unesp.br, henrique.leoncini@unesp.br, daniel.obata@unesp.br, jeferson.fukushima@unesp.br, amarildo.tabone@unesp.br

Abstract. *In recent years, the implementation of damping systems in civil structures has gained considerable attention, with emphasis on special building projects under dynamic loadings. In this scenario, due to their mechanical simplicity and controllable properties, Magneto-Rheological Elastomer (MRE) has stood out as providing an interesting alternative for vibration isolation. In these materials, the magnetic particles present in the elastomeric matrix are easily polarized in the presence of an external magnetic source, generating non-linear and reversible changes in the material, within a few milliseconds. In this way, the present work investigated numerically the efficiency of a certain damping system with MRE in isolating vibrations at the base of a bridge superstructure. The elastomer was simulated as a visco-elastic material of Kelvin-Voigt, and its stiffness and viscosity were regulated for five different scenarios. The unidimensional equivalent mechanical model was considered a single-degree-of-freedom (SDOF) system, and the ground motion generated by seismic excitations corresponded to shear excitations at the base. The base-isolated tests provided acceleration transmissibility under the different applied magnetic fields. It was observed that the viscoelastic support (VS) was able to shift the resonance frequency and the attenuation of transmissibility peak efficiently through field control. Moreover, with an adequate approach in the frequency domain, the random signal of a real earthquake was also inserted into the system for the evaluation of the isolator material. The finds demonstrated the good performance of the proposed MRE and its possibility of seismic vibrations mitigation.*

Keywords: *Magnetorheological elastomers, damping systems, vibration isolation.*

1. INTRODUCTION

A Bridge's structure can be divided into the superstructure, composed of deck and beams, mesostructure (columns), and infrastructure. Between the superstructure and mesostructure are locating bearings. According to Niemierko (2016), bearings are intermediate structural elements that help in the bridge's durability, reliability, and safety behavior. These devices are responsible for linking elements such as beams and pillars. In recent decades, a great development of modern structural designs for bearings can be observed, Block et al. (2013 *apud* Niemierko, 2016).

For this reason, smart materials have been integrated as bearings in the form of damping systems to optimize vibration isolation. Among these materials, Magneto-Rheological Elastomer (MRE) stands out, which is classified as a viscoelastic material (Jolly and Carlson, 2016), whose mechanical and rheological properties can be modified through the application of an external magnetic field (Bastola and Hossain, 2020). This classification of MRE as a viscoelastic material occurs because it presents characteristics between a viscous material and an elastic material when deformed. The elastic phase of the material is based on Hooke's law of isotropic elasticity and has no residual deformation, while, the viscous part is described by the Linear Law of Viscosity, defined by Newton. Thus, the graphic behavior of the MRE forms ellipsoidal curves showing slope, typical of elastic materials, and relaxation, typical of viscous materials.

Due to these properties, Tian and Nakano (2017) state that MREs have recently been used in a wide variety of applications, such as adapted vibration absorbers, dampers, sensors, and others. The damping occurs through the viscous flow of the rubber matrix and the inclusion of magnetic particles that allows additional, interfacial damping through the interaction of the particles (Khimi and Pickering, 2015). At first, it is necessary to incorporate a magnetic field source to change the characteristics of the MRE. Using a controllable source, particularly an electromagnetic component, the supply of electric current to the coil generates a magnetic field, increasing the stiffness of the elastomer. These changes are nonlinear, completely reversible, and occur in a few milliseconds (Ginder *et al*., 1999; Kukla *et al*., 2017).

First, to ensure the efficient insertion of this absorber, it is necessary to determine its internal forces and displacements, generally assuming that the structure is subjected to an arbitrary time-invariant load. One way to achieve this determination is ~~to~~ simplify the structure to perform a mechanical analysis, that is, to transform the structure into a system with n degrees of freedom (DOF) where the motion equations are obtained, thus enabling a prediction of the behavior along with some criteria such as natural frequency, stiffness, and damping. This is how this work intends to contribute to the studies of the present scenario.

This paper is organized as follows. Following this introduction, Section 2 describes the numerical modeling and procedures adopted for the simulation of the magneto-rheological elastomer. Exposure and discussion of the results are given in Section 3 and some conclusions are given in Section 4.

2. MATERIALS AND METHODS

2.1 Structure modeling

Due to the complexity of the real scale bridge system, this article uses only the structural form of a beam bridge to study the structure model with the vibration isolation system (Figure 1a). Therefore, a system of concentrated masses with a single degree of freedom (SDOF) was considered to model the superstructure and to analyze the similarity of the model with the best configuration of the MRE damper, as shown in Figure 1b.

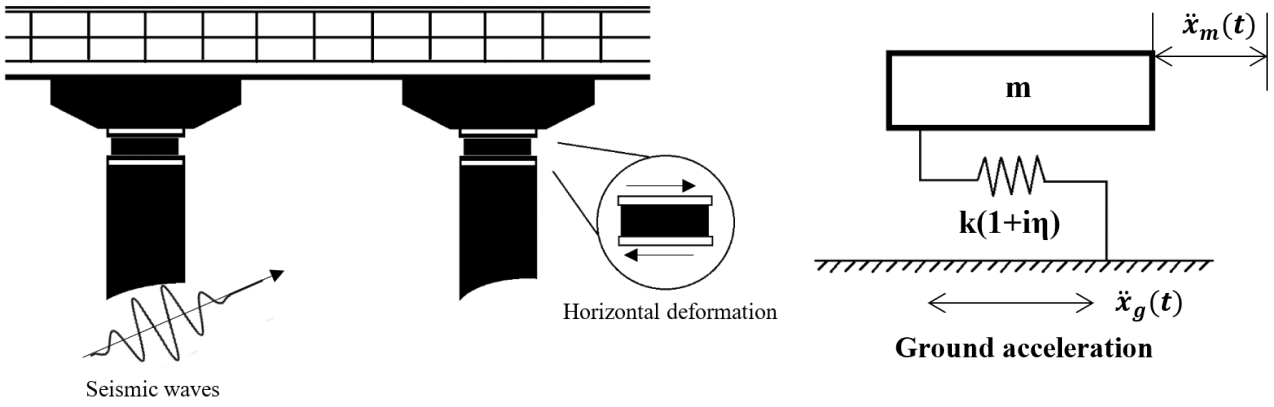

(a) (b)

Figure 1. a) Illustrative image of the bridge structure b) Mechanical system with viscoelastic damping.

The modeling starts with the description of the structure, considering its elements in a simplified way and the relationships between them. This set of elements forms the spatial model which has information on the mass and resistance of the system. An MRE model and stiffness elements will be included in the system to describe the dampers. Finally, it will be assumed that the structure suffers displacement only in the longitudinal direction of the superstructure, in a shear way. The excitation force generated causes a pure shear stress τ in the MRE sample which deforms at a displacement x, shown in Figure 2.

Consider a unidimensional system with single-degree-of-freedom of a viscoelastic material subjected to a harmonic force $F(t) = F_0.e^{j\omega t}$, as indicated in Figure 1b. The equation of motion of the inertial mass, m, can be described as:

$$m\ddot{x} + k(1 + j\eta)x = F_0 e^{j\omega t} \quad (1)$$

where k is the material's stiffness, η its viscosity and $k(1 + j\eta) = k^*$ is the complex stiffness.

The complex stiffness formulation is derived from the stress-strain relationship for a linear viscoelastic material, treated by Kelvin–Voigt rheological model.

$$\tau = G\gamma + \eta\,\dot{\gamma} \quad (2)$$

Shear stress in its basic form is given by the relationship between the applied force and the area that is sheared. Moreover, the stress can be deduced by the constitutive relation of the material, ie. the product of the shear modulus G and the angle γ generated by the displacement -. For small angles, it is assumed that its tangent is equal to the angle itself ($\tan\gamma = {}^{x}/_{h} \approx \gamma$). Therefore, making such manipulations, the stiffness k of the material is given as:

$$G = \frac{\tau_{xy}}{\gamma_{xy}} = \frac{F/A}{x/h} = \frac{k.h}{A} \quad ; \qquad k = \frac{G.A}{h} \tag{3}$$

where τ, F and A are the shear stress, force, and area, respectively, G, x, d h are the shear modulus, displacement, and sample length, respectively.

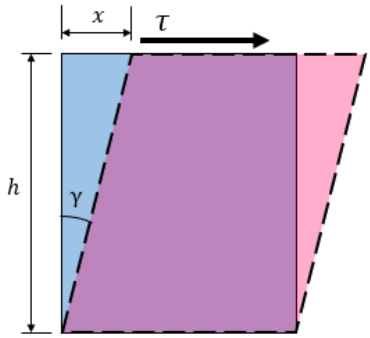

Figure 2. Deformation due to shear.

For the application of excitation, an earthquake signal was adopted to observe the behavior of the system when subjected to severe situations. The simulation was made with a real earthquake signal, which occurred in Iwate – Japan, in 2008. The signal was obtained from the PEER Ground Motion Database - NGA-West2 (2023) with a frequency within the range of 1 to 50Hz. Generally, an earthquake is referred to by its size, for this reason, magnitude scales such as the Richter scale are used. However, for engineering applications, the best way to analyze a seismic event is by the variation of acceleration or displacement of the ground in time. From this signal it is possible to extract parameters that will serve as a basis for understanding the behavior of an earthquake, considering, for example, its response spectrum.

2.2 MRE modeling

The magneto-rheological elastomer's bearing used as a reference has a matrix consisting of white silicone rubber high flexibility Redeleaser and has a concentration of 33% carbonyl iron magnetic particles (Sigma > 97%) with area A= 1200 x 1200mm and thickness e = 360mm – dimensions similar to those used by Block *et al.* (2013 *apud* Niemierko, 2016) for common elastomeric bearings. An inertial mass on the material m = 150kg was assumed, while the elastic and viscous properties of the MRE were obtained from a previous characterization carried out by Carvalho (2023), for shear stress of 0.49Pa, a frequency range between 10-60 Hz and field magnetic between 0.00 – 0.35 T. Tables 1 and 2 show the properties used.

Table 1. Values for Shear Modulus, G [MPa].

Magnetic fields [T]	**Frequency [Hz]**										
	10	**15**	**20**	**25**	**30**	**35**	**40**	**45**	**50**	**55**	**60**
0.00	0.534	0.567	0.588	0.597	0.595	0.601	0.607	0.609	0.606	0.608	0.604
0.07	0.636	0.673	0.683	0.699	0.701	0.713	0.716	0.725	0.732	0.733	0.745
0.14	0.864	0.913	0.921	0.953	0.958	0.983	0.996	1.026	1.032	1.029	1.041
0.21	1.212	1.248	1.271	1.304	1.305	1.341	1.330	1.325	1.324	1.327	1.290
0.28	1.698	1.810	1.836	1.890	1.879	1.890	1.873	1.876	1.864	1.858	1.873
0.35	2.142	2.303	2.392	2.429	2.397	2.395	2.405	2.424	2.420	2.428	2.427

Table 2. Values for the viscosity, η.

	Magnetic fields [T]					
	0.00	**0.07**	**0.14**	**0.21**	**0.28**	**0.35**
Viscosity [kPa.s]	1.8475	2.2081	3.1177	3.7668	4.9474	5.4649

3. RESULTS AND DISCUSSION

For each proposed arrangement, the absolute transmissibility was calculated (Eq. 4). The Motion Transmissibility Frequency Response Function is essential in vibration isolation studies since it defines the amount of motion transmitted from the base to the inertial mass, per unit of input motion in the support. Figure 3 and Figure 4 shows the results obtained.

$$Tr = k(1 + i\eta)/-m\omega^2 + k(1 + i\eta) \tag{4}$$

where k, η, m, and ω are stiffness, viscosity, mass, and angular frequency, respectively.

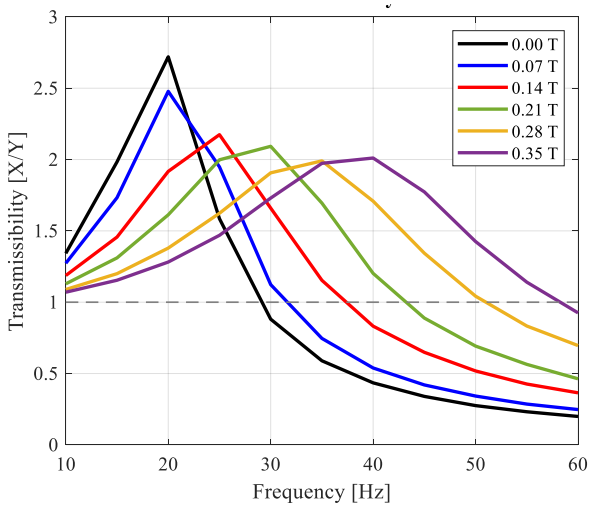

Figure 3. Absolute transmissibility of displacement for each magnetic field.

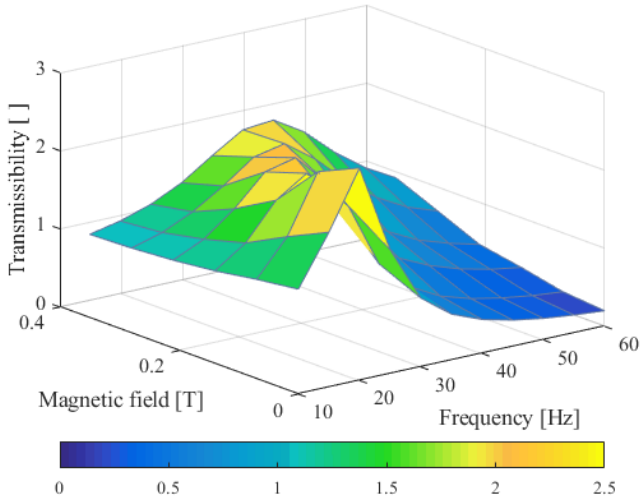

Figure 4. Transmissibility Surface.

As can be seen, changing the magnetic field can control the amplitude and frequency of the material's resonance peak. From 0.00 T to 0.35 T, the transmissibility was reduced by approximately 72%, and the resonance peak dropped from 20 Hz to 40 Hz.

In addition to directly influencing the region controlled by damping by changing the viscosity of the material, the imposed magnetic field changes its stiffness, thus controlling the region of resonances.

Analyzing the system's Transfer Function, shown in Figure 5 – the ratio between the output displacement and the input force (Eq. 5) – it is also possible to show the control action of the magnetic field on the simulated MRE.

It is important to point out that the geometric parameters of the MRE are also of great importance in the design of the insulators, because, as shown in Eq. (3), they directly influence the material stiffness.

$$H = 1/-m\omega^2 + k(1 + i\eta) \tag{5}$$

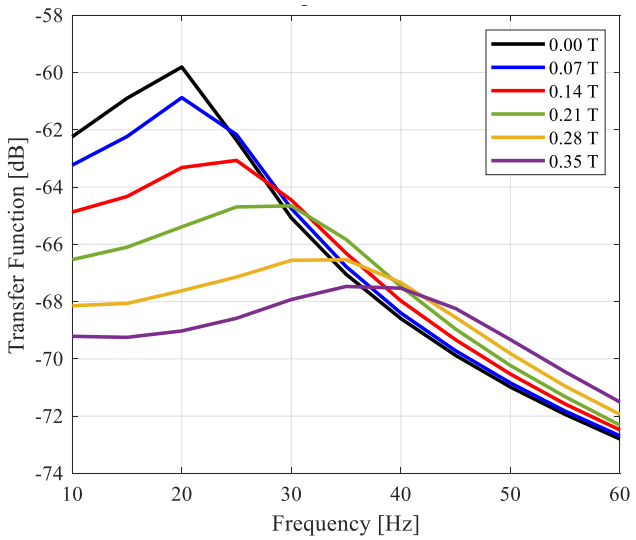

Figure 5. System Transfer Function H

Finally, to simulate a scenario close to reality, the random excitation of the collected real earthquake was inserted at the base of the insulator.

As depicted in Figure 1, it was assumed that the earthquake generates pure shear in the MRE. Figure 6 shows the applied earthquake displacement and Figure 7 presents the Fourier Transform of the signal.

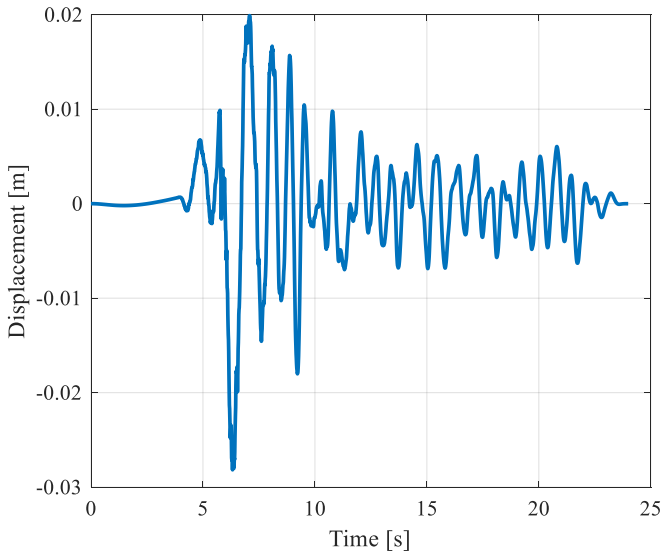

Figure 6. Time signal of the earthquake displacement.

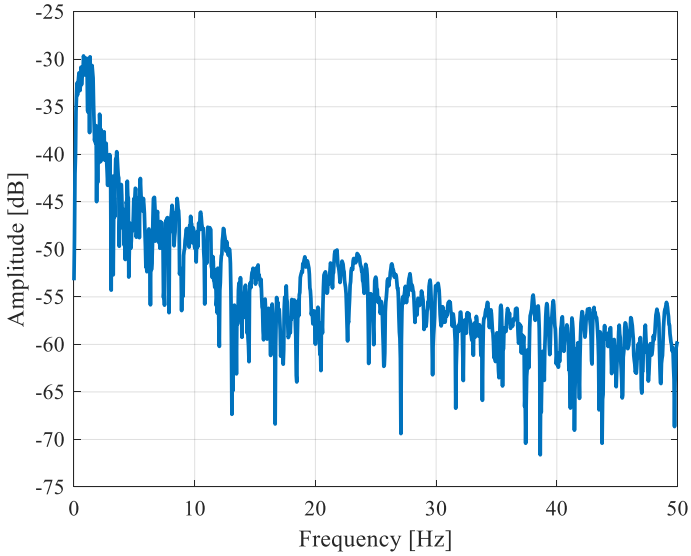

Figure 7. Earthquake signal FFT.

Figure 8 shows the influence of the magnetic field in controlling the system response. As can be seen, under the larger field, the peaks of the earthquake signal were reduced in the range of up to approximately 20 Hz. In contrast, the signal gained more amplitude at frequencies above 27 Hz.

The existing peaks between 19 and 24 Hz in the array devoid of field action, are due to the resonance region of the material for the case, as observed in Figures 3 and 4.

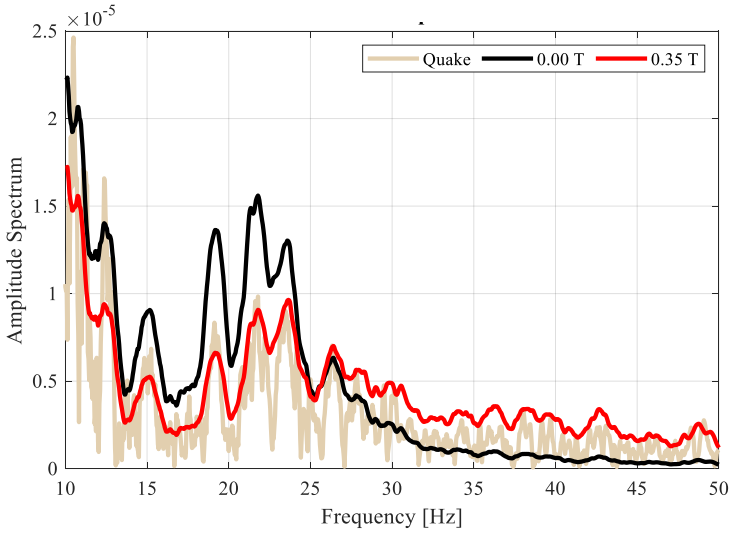

Figure 8. System response to real earthquake excitation under different magnetic fields.

4. CONCLUSION

From the results obtained, it can be concluded that the MRE was able to change its mechanical properties when subjected to an applied magnetic field, which showed a good agreement of data about the literature.

Larger magnetic fields are expected to further control the system's resonance peaks. Future research will characterize the elastic and viscous properties of the material for a wider frequency range and under higher magnetic fields, to better investigate the application of the material as a bridge insulator.

However, the previous results obtained already indicate that the material is a good candidate for the development of a damping system for bridges. Its advantage over current systems is the effective control of the magnetic field over its stiffness and damping.

5. ACKNOWLEDGEMENTS

This work was supported by the Coordination for the Improve of Higher Education Personnel (CAPES).

6. REFERENCES

Bastola, Anil K.; Hossain, Mokarram. A review on magneto-mechanical characterizations of magnetorheological elastomers. *Composites Part B: Engineering*, [S.L.], v. 200, p. 108348, nov. 2020. Elsevier BV.

Carvalho, Henrique E. L. Estudo do emprego de elastômero magneto-reológico para controle de vibrações em estruturas de engenharia civil. 2023. Tese (mestrado) – Universidade Estadual Paulista Júlio de Mesquita Filho, Faculdade de Engenharia de Ilha Solteira.

Ginder, John M. *et al*. Magnetorheological elastomers: properties and applications. *Smart Structures And Materials* 1999: Smart Materials Technologies, [s.l.], p.131-138, 12 Jul. 1999. SPIE. http://dx.doi.org/10.1117/12.352787.

Jolly MR, Carlson JD; MUNOZ BC. A model of the behavior of magnetorheological materials. *Smart Materials and Structures*, New York, v. 5, n. 5, p. 607–614, 1996.

Khimi, S. Raa; Pickering, K. l. Comparison of dynamic properties of magnetorheological elastomers with existing antivibration rubbers. *Composites Part B: Engineering*, Surrey, v. 83, n.1, p.175-183, dez. 2015. http://dx.doi.org/10.1016/j.compositesb.2015.08.033.

Kukla, Mateusz *et al*. The determination of mechanical properties of magnetorheological elastomers (MREs). *Procedia Engineering*, v. 177, n.1, p. 324-330, 2017. http://dx.doi.org/10.1016/j.proeng.2017.02.233.

Niemierko, Andrzej. Modern Bridge Bearings and Expansion Joints for Road Bridges. Transportation Research Procedia, [S.L.], v. 14, p. 4040-4049, 2016. Elsevier BV. http://dx.doi.org/10.1016/j.trpro.2016.05.501.

Pacific Earthquake Engineering Research Center. PEER Ground Motion Database. NGA West 2. https://ngawest2.berkeley.edu/site/documentation.

Tian, Tongfei; Nakano, Masami. Fabrication and characterization of anisotropic magnetorheological elastomer with 45° iron particle alignment at various silicone oil concentrations. Journal Of Intelligent Material Systems And Structures, [s.l.], v. 29, n. 2, p.151-159, 18 abr. 2017. SAGE Publications. http://dx.doi.org/10.1177/1045389x17704071.

7. RESPONSIBILITY NOTICE

The authors are the only ones responsible for the printed material included in this paper.